DAHLGREN DIVISION
NAVAL SURFACE WARFARE CENTER
Dahlgren, Virginia 22448-5100

NSWCDD/TN-97/190

TERMINAL GUIDANCE WITH A SIDE-MOUNTED SENSOR AGAINST A STATIONARY TARGET (U)

BY G. W. GROVES
SYSTEMS RESEARCH AND TECHNOLOGY DEPARTMENT

A. KHODARY
COMBAT SYSTEMS DEPARTMENT

DECEMBER 1997

FOREWORD

Installation of an additional sensor on the nose of a missile may require a complete redesign, whereas mounting on the side, away from the nose, may be relatively easy. However, use of a side-mounted sensor would require that the missile's heading error be sufficiently large, greater than a specified angle, in order that the sensor 'see' its target. This note examines the kinematics of flight, constrained in this way, for use against a stationary radiating target on the ground. If the missile is required to descend onto the target from above, for the purpose of continuous imaging the plan view of the target, an additional constraint is needed. Calculation of the miss distance achievable under different flight conditions is done to access the feasibility of a side-mounted sensor for this purpose.

The authors thank Frank Rucky for his encouragement and for suggesting this study; Ernest J. Ohlmeyer, Jr., Aeromechanics Branch, for his help and suggestions; and W. D. Blair and Greg Watson for their help and suggestions on track estimation. This work was funded through the Naval Surface Warfare Center, Dahlgren Division, Surface Weaponry Technology and Aegis Programs. This note has been reviewed by Dr. C. F. Fennemore, Technical Lead, Target Tracking and Signal Processing; Technology Program Manager, Robin Staton; and F. P. Rucky, Digital Systems Branch.

Approved by

Mary C Lacey

MARY E. LACEY, Head
Systems Research and Technology Department

ABSTRACT

Terminal guidance under the constraints that (*i*) the heading error must be greater than a specified angle (in order that the sensor see the target), and (*ii*) the magnitude of the lateral acceleration is limited, is studied. Only the kinematic features of flight are considered. It is demonstrated that a planar trajectory is as good as any for the purpose of hitting a stationary target on the ground. In order to hit, or come close to the target, the final segment of terminal flight must violate the heading-error constraint, during which time the target is invisible.

If there is an additional condition (*iii*) that the missile must remain above the target (*e.g.*, for imaging) during terminal descent, the optimum trajectory is a conic spiral. As in the previous case, there is a final segment of blind flight. The miss distance depends on the constraints and other parameters of the problem, as well as on the sensor measurement errors. Monte Carlo simulation was used to estimate the miss distance under various conditions.

CONTENTS

ILLUSTRATIONS

CHAPTER 1

INTRODUCTION

In passive homing, it is sometimes advantageous to place the sensor on the side of the missile or warhead (*e.g.*, on a ballistic warhead where placement on the nose would cause a difficult heating problem). However, a passive sensor on the side of the missile may prevent looking in the direction of motion. In such cases, an alternative homing technique where the missile velocity is constrained away from the look direction is required. A guidance law for the problem of engaging a quasi-stationary target on the ground by a vertically-descending side-looking missile is needed.

Aerodynamics is to be completely neglected. Thus, there is no missile body, and therefore no look direction relative to any body axis. The velocity vector essentially takes the place of the body axis and the heading error takes the place of the look angle. If the target is located at the origin, and $\underline{r}$ and $\dot{\underline{r}}$ denote the instantaneous missile position and velocity, while $\underline{r}_0$ and $\dot{\underline{r}}_0$ represent the initial values of these vectors, then the heading error ϕ is determined by

$$\cos\phi = -\frac{\underline{r}\cdot\dot{\underline{r}}}{rv} \tag{1.1}$$

(see Figure 1-1) where r stands for $|\underline{r}|$ and v stands for $|\dot{\underline{r}}|$. The placement of the sensor will make it impossible to 'see' the target if the look angle is too small. This constraint is expressed by requiring that the heading error ϕ never be less than a given critical angle ϕ_c.

In this simplified analysis it will be assumed that v remains constant. This is somewhat realistic if the missile is dropping toward the target in an almost vertical trajectory, in which case v will be approximately determined by the missile terminal speed. The terminal speed decreases with increasing air density, but this small effect is neglected. It will also be assumed that the missile is capable of only a limited lateral acceleration to be denoted by a_c, which may depend on the speed v.

It is likely that no trajectory will be able to actually *hit* the target under the reasonable conditions outlined below. If this is the case, the problem becomes one of approaching "near enough" to the target to destroy it with a proximity fuse, or to hit part of a large extended target. It may be necessary to specify another parameter, D_m, the maximum allowed miss distance whereby trajectories approaching within D_m of the target are deemed to be successful.

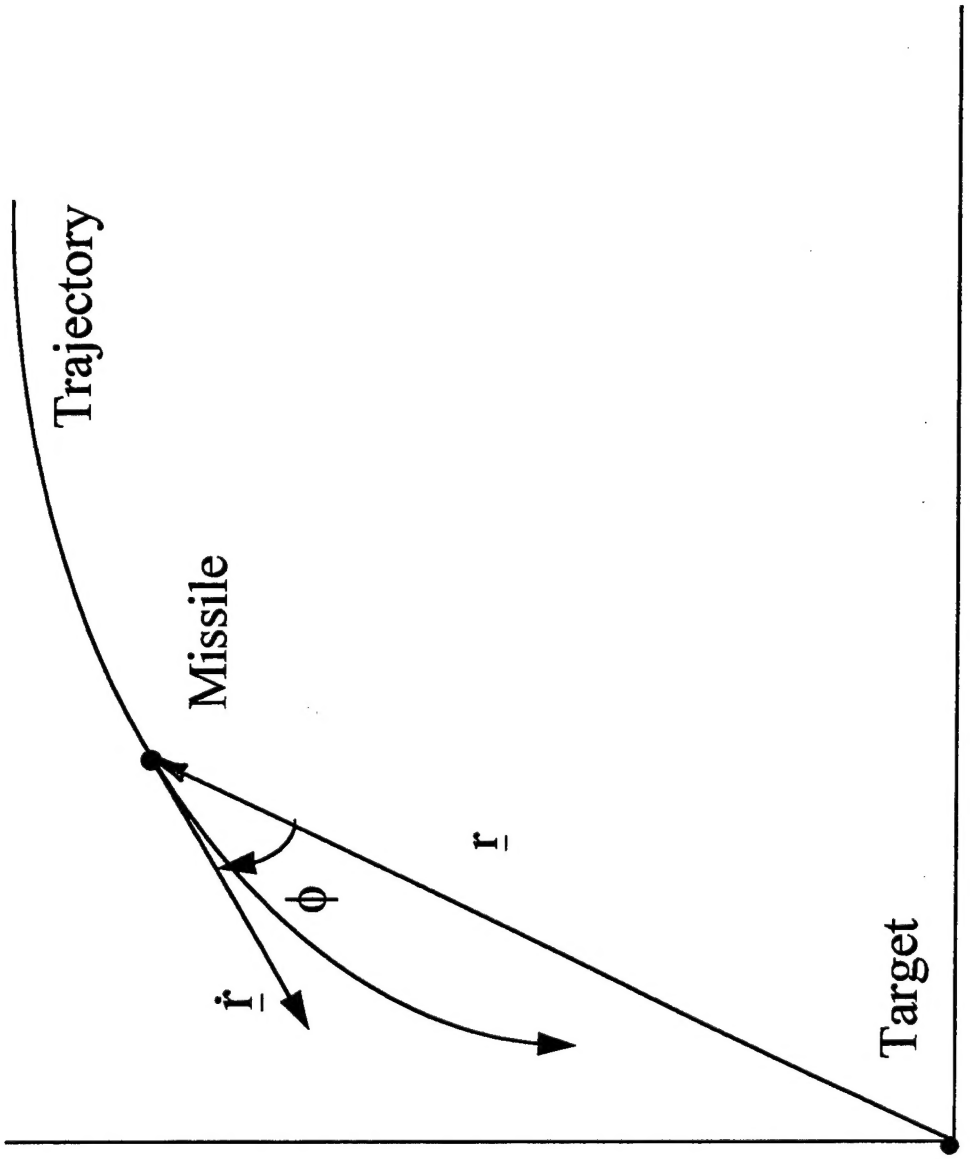

Figure 3-1. The Heading Error, ϕ.

CHAPTER 2

PLANAR TRAJECTORIES

This chapter considers the terminal flight phase during which the missile approaches the target along a planar trajectory. The flight previous to the terminal phase, in which the missile comes from a more distant launching point and arrives to the vicinity of the target, is not of interest and is not discussed. This preliminary flight phase can be governed by any guidance scheme including Proportional Navigation (PN), and is here referred to as the PN phase. The Heading Error (HE), denoted by ϕ, must always exceed a prescribed minimum value ϕ_c in order that the sensor see the target, as explained in Chapter 1.

In the approach (or PN) phase, the HE will generally decrease as the velocity vector tends to point closer and closer toward the target. As soon as the Heading Error (HE) becomes as small as ϕ_c, the trajectory will transition to Constant Heading Error (CHE). The reason for this is that increasing the HE, although allowed by the constraint, will degrade the trajectory and delay the arrival time in the deterministic case or increase the miss distance in stochastic cases.

During a CHE trajectory the lateral acceleration magnitude (LA) increases without limit as the turn radius decreases. This continual decrease in the turn radius is illustrated in Figures 2-1(a) and 2-1(b). Since the CHE trajectory will not approach near enough to the target without unlimited LA, there is a transition to a CLA (constant LA) trajectory, which is a circular arc. During this final CLA trajectory the HE is generally too small for the target to be visible to the sensor, meaning that the missile is flying blind during the terminal CLA phase.

Let a_{CLA} be the LA required for the missile in its current state to transition to a CLA trajectory and hit the target. The logic determining the type of trajectory required can be expressed by the following algorithm:

while LA $< a_c/2$
  while $\phi > \phi_c$
    use PN (or any appropriate approach guidance)
  when $\phi = \phi_c$
    use CHE
  if $\phi < \phi_c$
    This condition should ordinarily never be encountered.
  end
when LA $= a_c/2$

transition to CLA, whereupon LA becomes equal to a_c

end

TRAJECTORY SHAPE

It is shown below that the planar trajectory is as good as any, for the purpose that has been described. Other considerations make the conic spiral (CS) trajectory advantageous (see Chapter 3).

Since it is evident that both the PN and CLA trajectories can be taken as planar, the following discussion is limited to a demonstration that the planar CHE trajectory is as good as any other CHE trajectory:

Writing (1.1) in the form

$$(\underline{r} \cdot \dot{\underline{r}})^2 = (vr\cos\phi)^2 = (v\cos\phi)^2(\underline{r} \cdot \underline{r}) \tag{2.1}$$

and differentiating with respect to time, one obtains

$$\underline{r} \cdot \ddot{\underline{r}} = -v^2\sin^2\phi \tag{2.2}$$

Let us find the most general acceleration that determines a constant-speed CHE trajectory as determined by the conditions

$$v = v_0, \qquad \phi = \phi_0 \tag{2.3}$$

Let the acceleration be expressed in the form

$$\ddot{\underline{r}} = A\underline{r} + B\dot{\underline{r}} + C\underline{n} \tag{2.4}$$

where A, B, and C are constants to be determined, and $\underline{n}$ is a unit vector perpendicular to the plane of $\underline{r}$ and $\dot{\underline{r}}$. It is possible to express an arbitrary vector in the form (2.4) because the base vectors used span the three-dimensional space except in the trivial case where $\underline{r}$ is parallel to $\dot{\underline{r}}$. The conditions (2.2) and $\dot{\underline{r}} \cdot \ddot{\underline{r}} = 0$ lead to the equations

$$\begin{aligned} r^2A - (vr\cos\phi)B &= -v^2\sin^2\phi \\ -(vr\cos\phi)A + v^2B &= 0 \end{aligned} \tag{2.5}$$

that determine A and B, where v and ϕ are constants according to the constant-speed and CHE hypotheses (2.3). The acceleration resulting from the values of A and B determined by (2.5) is

$$\ddot{\underline{r}} = -r^{-2}[v^2\underline{r} + (vr\cos\phi)\dot{\underline{r}})] + C\underline{n} \tag{2.6}$$

This is the most general form for the acceleration that satisfies both the constant-speed and the CHE conditions. The 'constant' C has not been determined, and it can take any value at any time. The LA magnitude is

$$|\ddot{\underline{r}}| = \sqrt{v^4r^{-2}\sin^2\phi + C^2} \tag{2.7}$$

If the optimum CHE trajectory is defined as that trajectory which obeys both the constant-speed and CHE conditions and requires the minimum LA at each instant, then (2.7) shows that this trajectory is planar with the constant C identically zero.

In the CHE trajectory, all permissible accelerations give the same rate of approach to the target, namely, $\dot{r} = -v\cos\phi_c$. However, the acceleration that lies on the plane of $(\underline{r}, \dot{\underline{r}})$ has the smallest magnitude $|\ddot{\underline{r}}|$ as shown by (2.7). In the CLA part of the trajectory, the acceleration that lies on this same plane gives the largest rate of approach to the target.

Consider now the LA required for the missile to transition from its current state to a CLA trajectory that intersects the target. Simple geometry shows that this LA is given by

$$a_{CLA} = \frac{2v^2}{r}\sin\phi \tag{2.8}$$

which is just twice the value of $|\ddot{\underline{r}}|$ needed to maintain a CHE trajectory, as shown by (2.7) with $C = 0$. Accordingly, at all times during a CHE trajectory, the LA being applied in order to maintain the CHE trajectory is just half that required to transition to a terminal CLA trajectory that hits the target. Upon transition to the CLA trajectory, the LA is abruptly doubled.

The dependence of velocity on range in the CHE trajectory can be found by expressing it as a linear combination of $\underline{r}$ and $\underline{k}$, the unit upward vector. The condition (1.1) along with the requirement that the velocity magnitude equal v gives

$$\dot{\underline{r}} = \pm[r^2 - (\underline{k}\cdot\underline{r})^2]^{-1/2}[-r^{-1}(\underline{k}\cdot\underline{r})\underline{r} + r\underline{k}]v\sin\phi_c - vr^{-1}\underline{r}\cos\phi_c \tag{2.9}$$

The trajectory shape is easily found in polar coordinates (r, θ) on the flight plane, in terms of which the (constant) speed is given by

$$v = \sqrt{\dot{r}^2 + r^2\dot{\theta}^2} \tag{2.10}$$

while the condition (1.1) becomes

$$\dot{r} = v\cos\phi_c \tag{2.11}$$

Equations (2.10) and (2.11) determine the trajectory in the form $\theta(r)$, where

$$\theta(r) = \theta_0 - (\tan\phi_c)\ln(r/r_0) \tag{2.12}$$

with θ_0 representing the polar angle where the range is r_0. Some typical CHE trajectories are shown in Figures 2-1 and 2-2.

In an actual engagement, the missile flies to the vicinity of the target during the initial flight phase during which the HE generally decreases continually. When the HE becomes as small as ϕ_c there is transition to a CHE trajectory during which the LA continually increases. But before the LA becomes as large as a_c there must be another transition to a

CLA trajectory. This is because there is an abrupt increase in the LA upon this transition, and it is the increased LA during the terminal CLA trajectory that intersects the target that must be constrained to not exceed a_c.

Figure 2-3 illustrates a hypothetical sequence of these events on a plot of lateral acceleration against HE. During PN both the LA and the HE generally decrease. When the HE reaches the value ϕ_c there is transition to CHE, because otherwise the target would not be visible to the sensor. During CHE the LA increases until half the limiting value is reached, whereupon there is transition to the terminal CLA trajectory. At this transition the LA abruptly increases by a factor of two.

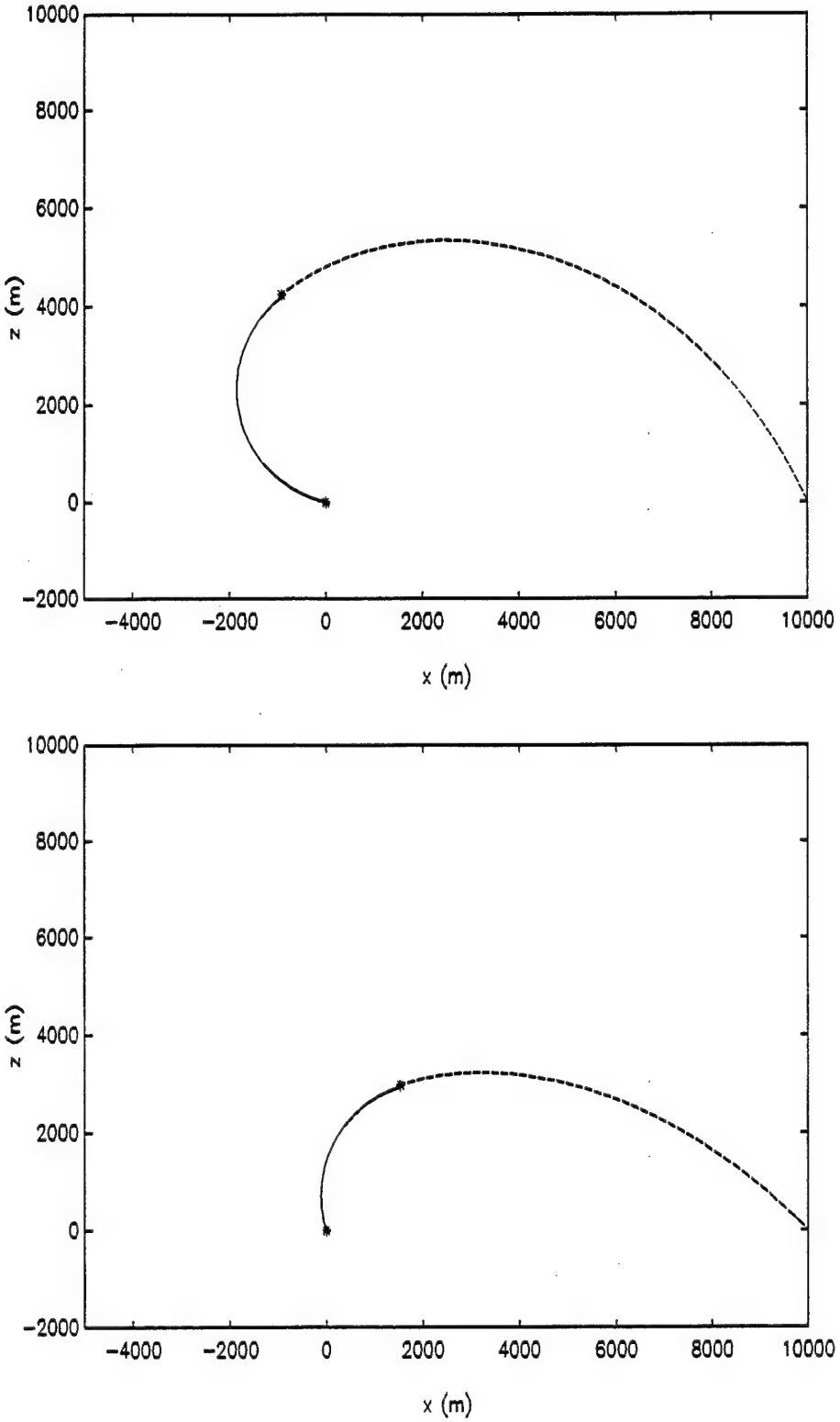

Figure 2-1 (a) above; (b) below; Typical CHE trajectories (dashed) with terminal CLA trajectories (solid). Target and transition points are marked with stars. The curvature (and LA) abruptly doubles at the transition points.

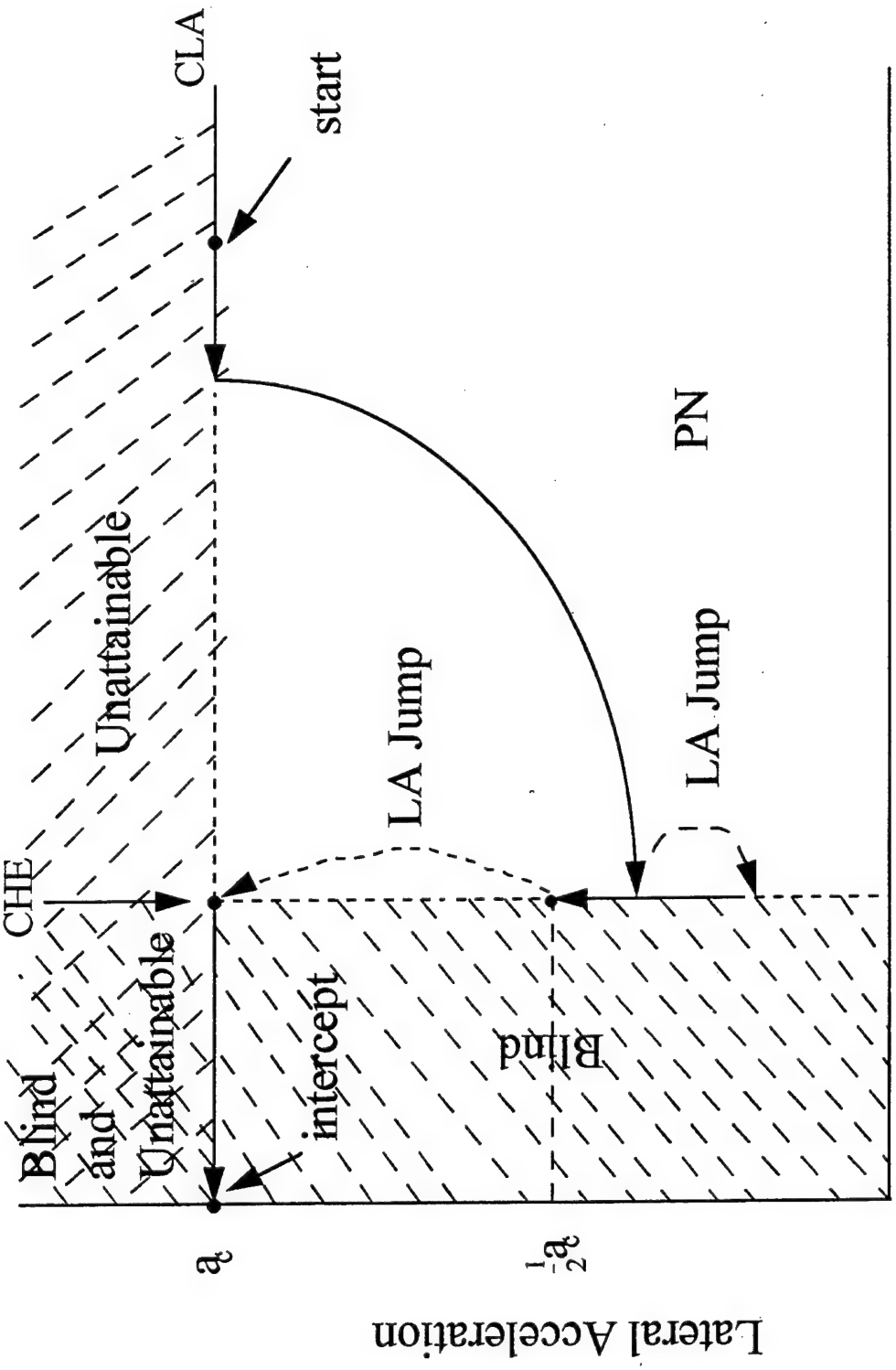

Figure 2-2. Hypothetical Evolution of Trajectory.

CHAPTER 3

APPROACH FROM ABOVE

Consider now the case where it is deemed desirable to approach the stationary target from above. Such a quasi-vertical approach is advantageous when a view of the target is to be compared with an image as viewed from above. A strictly vertical approach is impossible. Let an angular deviation from the vertical, α, be defined. The flight of the missile is to be constrained to lie within a circular cone, $\alpha \leq \alpha_c$, for specified α_c. The axis of this cone is vertical and its apex is located at the target. A heuristic argument indicates that the best trajectory lies *on* the cone. Discussion of the initial flight segment that brings the missile to the beginning of the "conic spiral" (CS) is deferred.

Let the motion be described in terms of new position coordinates (ρ, θ, α). The relation between these and the Cartesian coordinates is

$$\begin{aligned} x &= \rho \cos\theta \\ y &= \rho \sin\theta \\ z &= \rho \operatorname{ctn}\alpha \end{aligned} \tag{3.1}$$

The inverse relation is given by

$$\begin{aligned} \rho &= \sqrt{x^2 + y^2} \\ \theta &= \arctan(y/x) \\ \alpha &= \arctan(\sqrt{x^2 + y^2}/z) \end{aligned} \tag{3.2}$$

From now on, α is taken to be constant and equal to α_c. The velocity components are given by

$$\begin{aligned} \dot{x} &= \dot{\rho}\cos\theta - \rho\dot{\theta}\sin\theta \\ \dot{y} &= \dot{\rho}\sin\theta + \rho\dot{\theta}\cos\theta \\ \dot{z} &= \dot{\rho}\operatorname{ctn}\alpha - \rho\dot{\alpha}\csc^2\alpha \end{aligned} \tag{3.3}$$

The HE is denoted by ϕ, which is given by the relation

$$\cos\phi = -\frac{\underline{r}\cdot\dot{\underline{r}}}{rv} \tag{3.4}$$

Let us now examine the motion governed by the conditions $\phi = \phi_c$ and $\alpha = \alpha_c$, where ϕ_c and α_c are specified constants. Then (3.4) gives

$$\dot{\rho} = -v\cos\phi_c \sin\alpha_c \tag{3.5}$$

Using (3.3) and (3.5), the velocity components can be written

$$\begin{aligned} \dot{x} &= -v\cos\phi_c\sin\alpha_c\cos\theta - z\dot{\theta}\tan\alpha_c\sin\theta \\ \dot{y} &= -v\cos\phi_c\sin\alpha_c\sin\theta + z\dot{\theta}\tan\alpha_c\cos\theta \\ \dot{z} &= -v\cos\phi_c\cos\alpha_c \end{aligned} \tag{3.6}$$

The requirement that (3.6) represent a constant speed v gives

$$\dot{\theta}^2 = \frac{v^2 \sin^2 \phi_c}{z^2 \tan^2 \alpha_c} \tag{3.7}$$

from which θ becomes

$$\theta = \pm \frac{v \sin \phi_c}{z \tan \alpha_c} t \tag{3.8}$$

The $\pm$ sign indicates that the missile can spiral in either the clockwise or counterclockwise direction. Using this result, the velocity components can be expressed as a function of position, becoming

$$\begin{aligned} \dot{x} &= vz^{-1}(-x \cos \phi_c \cos \alpha_c \mp y \sin \phi_c \operatorname{ctn} \alpha_c) \\ \dot{y} &= vz^{-1}(-y \cos \phi_c \cos \alpha_c \pm x \sin \phi_c \operatorname{ctn} \alpha_c) \\ \dot{z} &= -v \cos \phi_c \cos \alpha_c \end{aligned} \tag{3.9}$$

The upper (or lower) signs should be used consistently throughout. The acceleration components can be obtained as functions of position by differentiating (3.9), becoming

$$\begin{aligned} \ddot{x} &= v^2 z^{-2}(\pm y \cos \phi_c \sin \phi_c \cos \alpha_c \operatorname{ctn} \alpha_c - x \sin^2 \phi_c \operatorname{ctn}^2 \alpha_c) \\ \ddot{y} &= v^2 z^{-2}(\mp x \cos \phi_c \sin \phi_c \cos \alpha_c \operatorname{ctn} \alpha_c - y \sin^2 \phi_c \operatorname{ctn}^2 \alpha_c) \\ \ddot{z} &= 0 \end{aligned} \tag{3.10}$$

The acceleration vector $\ddot{\underline{r}}$ lies on the horizontal plane and is perpendicular to the velocity vector. Its magnitude is

$$|\ddot{\underline{r}}| = v^2 z^{-1} \sin \phi_c \operatorname{ctn} \alpha_c \sqrt{\cos^2 \phi_c \sin^2 \alpha_c + \sin^2 \phi_c} \tag{3.11}$$

The integral of the motion gives the time history of the trajectory,

$$\begin{aligned} z &= z_0 - vt \cos \phi_c \cos \alpha_c \\ \theta &= \theta_0 \pm \frac{\tan \phi_c}{\sin \alpha_c} \ln \left(1 - \frac{v \cos \phi_c \cos \alpha_c}{z_0} t \right) \end{aligned} \tag{3.12}$$

This is the CS. It appears that this simplistic and purely kinematic discussion may work well. In particular, the constant v assumption may not be overly far-fetched. It is noted that constant power is being received by the missile from its uniformly-diminishing potential energy.

THE BLIND FLIGHT PLANE (BFP)

As before, it is impossible to hit the target with finite LA capability. Therefore, a maximum LA value of a_c is specified. At some point, a transition is made to a constant LA trajectory (CLA) that will intersect the target. During this CLA trajectory the HE may become less than ϕ_c, meaning that the missile flies blind.

Let θ_1 be the polar angle at the point of transition. The target and the velocity at the point of transition lie on the cone, and also on a plane to be called the BFP, which is tangent

to the cone along the line $\theta = \theta_1$. Let (ξ, η) be Cartesian coordinates on the BFP, with the η direction being generally upward. The relations between the BFP coordinates and the original three-dimensional Cartesian coordinates are given by

$$\begin{aligned} x &= \eta \sin\alpha \cos\theta_1 - \xi \sin\theta_1 \\ y &= \eta \sin\alpha \sin\theta_1 + \xi \cos\theta_1 \\ z &= \eta \cos\alpha \end{aligned} \tag{3.13}$$

Matching the three Cartesian components of velocity at the transition point, indicated by the subscript "1", gives the relations

$$\begin{aligned} \dot{\eta}_1 \sin\alpha_c \cos\theta_1 - \dot{\xi} \sin\theta_1 &= \dot{\rho}_1 \cos\theta_1 - \rho_1 \dot{\theta}_1 \sin\theta_1 \\ \dot{\eta}_1 \sin\alpha_c \sin\theta_1 + \dot{\xi}_1 \cos\theta_1 &= \dot{\rho}_1 \sin\theta_1 + \rho_1 \dot{\theta}_1 \cos\theta_1 \\ \dot{\eta}_1 &= \dot{\rho}_1 \csc\alpha_c \end{aligned} \tag{3.14}$$

The acceleration at transition is not matched because it can abruptly change. The terminal CLA trajectory begins at $(\xi, \eta) = (0, \eta_1)$ and ends at $(\xi, \eta) = (0, 0)$. Matching the trajectory slope m on the (ξ, η) plane at transition gives

$$|m| = \frac{\dot{\eta}_1}{|\dot{\xi}_1|} = \frac{\dot{\rho}_1 \csc\alpha_c}{\rho_1 |\dot{\theta}_1|} \tag{3.15}$$

The geometry of the circular arc on the (ξ, η) plane shows that the initial η must be given by

$$\eta_1 = \frac{2v^2}{a_b} \sin\phi_c \tag{3.16}$$

in order that the missile trajectory hit the target, where a_b is the constant LA on the BFP.

On the cone the flight is governed by the relation $\phi = \phi_c$, while on the BFP the flight is governed by the relation $a = a_b$. According to (3.11) the LA on the cone at transition is given by

$$a_m = \frac{v^2 \sin\phi_c \csc\alpha_c}{\eta_1} \sqrt{\cos^2\phi_c \sin^2\alpha_c + \sin^2\phi_c} \tag{3.17}$$

The HE, ϕ, during flight on the BFP obeys the relation

$$\frac{2v^2}{a_b} \cos(\phi_c - \phi) \sin\phi = \eta \tag{3.18}$$

from which it is seen that

$$\frac{\partial \eta}{\partial \phi} = \frac{2v^2}{a_b} \cos(\phi_c - 2\phi) \tag{3.19}$$

Since η monotonically decreases in the BFP, while the right side of (3.19) is always positive in the appropriate domain of the variables, ϕ continually decreases. Thus, the condition $\phi \geq \phi_c$ is immediately violated upon transition to the BFP, and the entire flight from transition is

blind. In addition, the missile immediately leaves the cone upon transition and even if the target were to remain visible, it would not be sufficiently 'below' the missile.

The constraint on LA requires that $a_m \leq a_c$ and $a_b \leq a_c$. Considering (3.15) and (3.16), these conditions provide the following rule by which the distance of blind flight, η_1, in the BFP is determined. Define the ratio

$$\mu = \frac{a_m}{a_b} = \frac{1}{2}\sqrt{\cos^2\phi_c + \left(\frac{\sin\phi_c}{\sin\alpha_c}\right)^2} \tag{3.20}$$

The value $\mu = 1$ marks the transition from one criterion to the other. Let $\alpha = \alpha_1$ be the value for which $\mu = 1$ for given ϕ_c. This value is given by the relation

$$\sin\phi_c = \sqrt{3}\tan\alpha_1 \tag{3.21}$$

Then

$$\text{if} \quad \alpha \geq \alpha_1, \quad \rightarrow \quad \mu \leq 1, \quad \rightarrow \quad a_b = a_c, \quad \rightarrow \quad \eta_1 = \frac{2v^2}{a_c}\sin\phi_c \tag{3.22}$$

$$\text{if} \quad \alpha \leq \alpha_1, \quad \rightarrow \quad \mu \geq 1, \quad \rightarrow \quad a_b = a_c/\mu, \quad \rightarrow \quad \eta_1 = \frac{2v^2\mu}{a_c}\sin\phi_c \tag{3.23}$$

The miss distance is determined by the conditions at transition between the CS and the BF trajectory, because after the transition no further measurements are possible. The position $\underline{r}_1$ and velocity $\dot{\underline{r}}_1$ at transition are the final values in the CS trajectory. The subsequent flight is along a circular arc with center at $\underline{r}_c$, where $\underline{r}_c$ lies in the plane of the missile position and velocity. Therefore, express $\underline{r}_c$ in the form

$$\underline{r}_c = A\underline{r}_1 + B\dot{\underline{r}}_1 \tag{3.24}$$

where A and B are constants to be determined. Also, let $\dot{\underline{r}}_f$ be the final velocity at the target. This final velocity is determined by the conditions $\dot{\underline{r}}_1 + \dot{\underline{r}}_f = -C\underline{r}_1$;, where C is a positive constant, and $|\dot{\underline{r}}_f| = |\dot{\underline{r}}_1| = v$. Under these conditions, the final velocity is given by

$$\dot{\underline{r}}_f = 2\frac{\underline{r}_1 \cdot \dot{\underline{r}}_1}{r_1^2}\underline{r}_1 - \dot{\underline{r}}_1 \tag{3.25}$$

The center of curvature is determined by the conditions $r_c = |\underline{r}_1 - \underline{r}_c| = b$, $\underline{r}_c \cdot \dot{\underline{r}}_f = 0$, and $(\underline{r}_1 - \underline{r}_c) \cdot \dot{\underline{r}}_1 = 0$. These conditions require that

$$\underline{r}_c = A\underline{r}_1 + \frac{(1-A)\underline{r}_1 \cdot \dot{\underline{r}}_1}{v^2}\dot{\underline{r}}_1 \tag{3.26}$$

where A is given by

$$A = \frac{v^2 r_1^2 - 2(\underline{r}_1 \cdot \dot{\underline{r}}_1)^2}{2[v^2 r_1^2 - (\underline{r}_1 \cdot \dot{\underline{r}}_1)^2]} \tag{3.27}$$

Accordingly, the radius of curvature is

$$b = \frac{v r_1^2}{2\sqrt{v^2 r_1^2 - (\underline{r}_1 \cdot \dot{\underline{r}}_1)^2}} \tag{3.28}$$

while the required acceleration just after transition is given by

$$\ddot{\underline{r}}_1 = \frac{\underline{r}_c - \underline{r}_1}{b} |\ddot{\underline{r}}_1| = \frac{2v^2}{r_1^2} \left(-\underline{r}_1 + \frac{\underline{r}_1 \cdot \dot{\underline{r}}_1}{v^2} \dot{\underline{r}}_1 \right) \tag{3.29}$$

and its magnitude is

$$|\ddot{\underline{r}}_1| = \frac{2v^2}{r_1^2} \sqrt{r_1^2 - \frac{(\underline{r}_1 \cdot \dot{\underline{r}}_1)^2}{v^2}} \tag{3.30}$$

If the true missile state at transition were known, its subsequent flight would be given by

$$\underline{r}(t) = \underline{r}_1 + \dot{\underline{r}}_1 \omega^{-1} \sin \omega t + \ddot{\underline{r}}_1 \omega^{-2} (1 - \cos \omega t) \tag{3.31}$$

(see Groves et al, 1994), where

$$\omega = \frac{|\ddot{\underline{r}}_1|}{|\dot{\underline{r}}_1|} \tag{3.32}$$

This trajectory passes through the origin. That is, under these supposed conditions of knowledge of the true missile state at transition, the missile hits the target. If the true missile state at transition is known only approximately, the acceleration to be applied to the missile at each instant is given by the derivative of (3.31),

$$\ddot{\underline{r}}(t) = -\dot{\underline{r}}_1 \omega \sin \omega t + \ddot{\underline{r}}_1 \cos \omega t \tag{3.33}$$

This acceleration is computed from the estimated target state at transition and applied to the true state, in timestepping, until the missile altitude reaches zero, whereupon the miss distance is given by the horizontal missile position on the plane $z = 0$.

Figure 3-1 shows a typical CS trajectory projected onto the horizontal plane. Figure 3-2 shows the projection of the same trajectory onto a vertical plane.

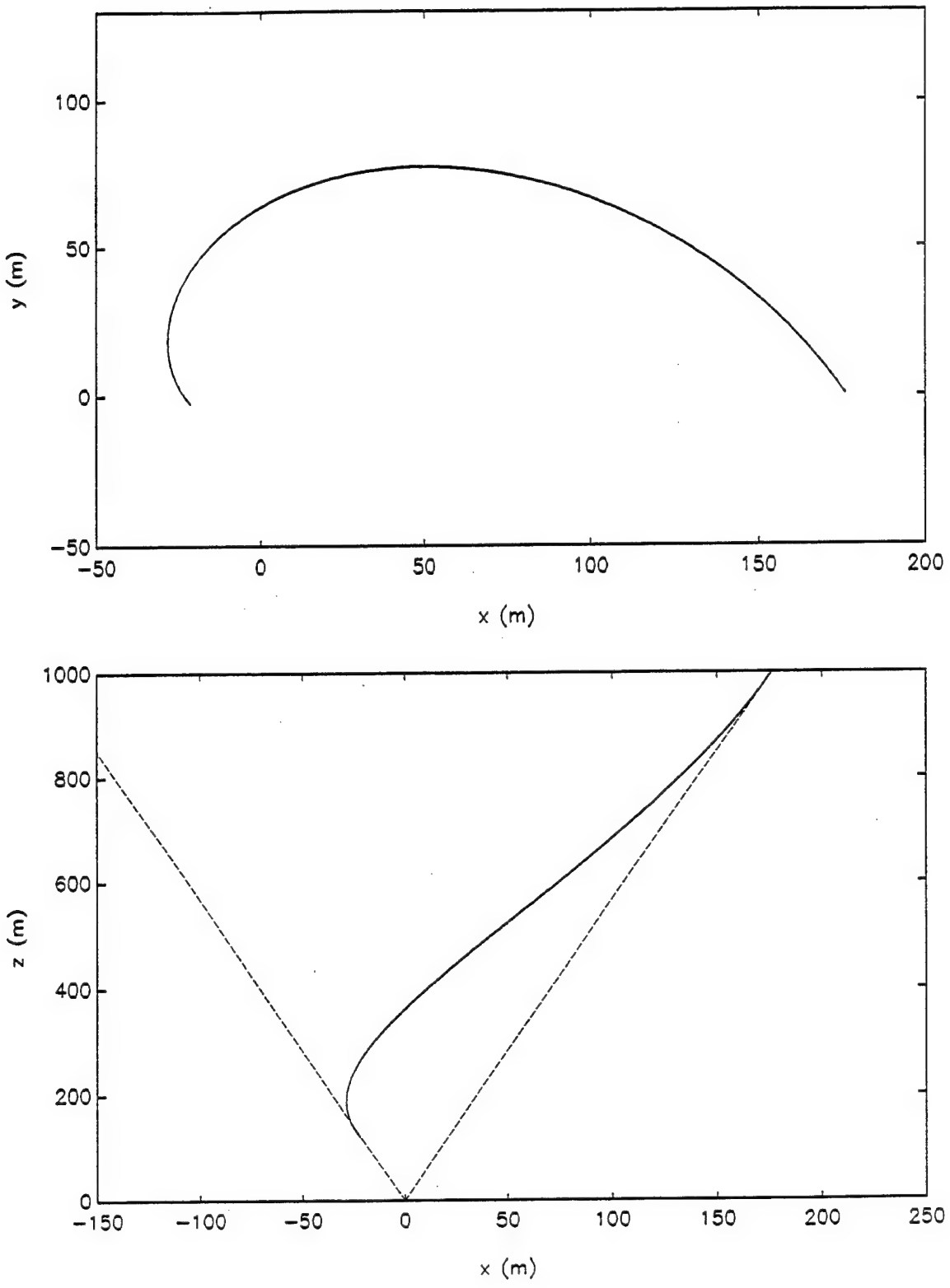

Figure 3-1. A typical conic-spiral trajectory. Upper plot – projection on horizontal plane: Lower plot – projection on (x,z) plane.

CHAPTER 4

GUIDANCE USING STATE ESTIMATION BY THE KALMAN FILTER

The Kalman Filter is a general solution to the minimized mean square estimation problem for a linear dynamic system. The Kalman Filter gives a minimum error variance recursive algorithm to estimate an instantaneous state of a linear model system by using a measurement linearly related to the state, but corrupted by Gaussian white noise taken at discrete time intervals. For a Gaussian random variables, the Kalman Filter provides the minimum mean-square error estimate of the state and for variables of forms other than Gaussian, the Kalman Filter is the best linear estimator of the state in the mean square error sense.

To provide the appropriate acceleration commands (3.10) for the missile to execute the CS trajectory, an estimate of the missile position at each instant is required. The procedure is to first apply a time update to estimate the missile state at a future time given its current state. Then a measurement update is applied. The time update is usually based on a simple extrapolation scheme, such as the assumption that the missile velocity will remain constant during the extrapolation interval. This is the constant velocity (CV) update. In the CS trajectory, a time update using a Constant-Turning-Rate assumption will make the measurement innovations smaller and lead to smaller estimation errors. The model of Blair et al (1997) is used, based on the Constant-Turning-Rate trajectory of Groves et al (1994).

The linear dynamic model commonly used for a target in track is represented by

$$X_k = F_{k-1}X_{k-1} + G_{k-1}w_{k-1} \tag{4.1}$$

where X_k represents the states of the target at time k. For the constant Turn-Rate model, the elements of X_k are position (x, y, z), velocity $(\dot{x}, \dot{y}, \dot{z})$ and acceleration $(\ddot{x}, \ddot{y}, \ddot{z})$, $w_k \sim N(0, Q_k)$ is the process noise, assumed Gaussian, and F_k and G_k define the dynamics of the target. The linear measurement process is given by

$$Z_k = H_k X_k + v_k \tag{4.2}$$

(see, for example, Gelb, 1974) where Z_k is the discrete-time measurement at time k, $v_k \sim N(0, R_k)$ is the measurement noise, assumed Gaussian, and H_k is a matrix relating the target state to the measurements.

Implementation of the standard Kalman Filter algorithm requires that both the states and the measurement models be linear. For the linear system prescribed by Equations (4.1) and (4.2), the standard Kalman Filter algorithm is given by

I. Time Update:

$$X_{k|k-1} = F_{k-1}X_{k-1|k-1} \tag{4.3}$$

$$P_{k|k-1} = F_{k-1}P_{k-1|k-1}F_{k-1}^T + G_{k-1}Q_{k-1}G_{k-1}^T \tag{4.4}$$

II. Measurement Update:

$$X_{k|k} = X_{k|k-1} + K_k(Z_k - H_kX_{k|k-1}) \tag{4.5}$$

$$P_{k|k} = (I - K_kH_k)P_{k|k-1} \tag{4.6}$$

$$K_k = P_{k|k-1}H_k^T(H_kP_{k|k-1}H_k^T + R_k)^{-1} \tag{4.7}$$

where $X_{k|k}$ is the state estimate at time k, $P_{k|k}$ is the error covariance matrix at time k, and K_k is the Kalman gain at time k. The vector $X_{k|k-1}$ represents the predicted state estimate at time k based on measurements through time $k-1$. and $P_{k|k-1}$ represents the covariance at time k based on measurements through time $k-1$.

The discrete-time dynamics for constant turn-rate model is given by (4.1) with

$$F_k = \begin{pmatrix} A_k & 0 & 0 \\ 0 & A_k & 0 \\ 0 & 0 & A_k \end{pmatrix}, \qquad G_k = \begin{pmatrix} B_k & 0 & 0 \\ 0 & B_k & 0 \\ 0 & 0 & B_k \end{pmatrix} \tag{4.8}$$

where

$$A_k = \begin{pmatrix} 1 & \omega^{-1}\sin(\omega T) & \omega^{-2}(1-\cos(\omega T)) \\ 0 & \cos(\omega T) & \omega^{-1}\sin(\omega T) \\ 0 & -\omega\sin(\omega T) & \cos(\omega T) \end{pmatrix},$$

$$B_k = \begin{pmatrix} \frac{1}{6}T^3 & \frac{1}{2}T^2 & T \end{pmatrix}^T \tag{4.9}$$

$$X_k = \{x\ \dot{x}\ \ddot{x}\ y\ \dot{y}\ \ddot{y}\ z\ \dot{z}\ \ddot{z}\}_k^T \tag{4.10}$$

where T is the time interval between measurements k and $k+1$, and $\omega = |\underline{\ddot{r}}|/|\underline{\dot{r}}|$.

Following Ohlmeyer (1985), we assume that the discrete measurements are available in a nonlinear function of the state X_k, and are represented by:

$$Z_k = h_kX_k + v_k \tag{4.11}$$

where

$$Z_k = \begin{pmatrix} \text{range} \\ \text{azimuth angle} \\ \text{elevation angle} \end{pmatrix}$$

$$h_k(X_k) = \begin{pmatrix} \sqrt{(x_k^2 + y_k^2 + z_k^2)} \\ \arctan(y_k/x_k) \\ \arctan\left(z_k/\sqrt{x_k^2 + y_k^2}\right) \end{pmatrix}, \qquad v_k = \begin{pmatrix} v^r \\ v^b \\ v^e \end{pmatrix}_k \tag{4.12}$$

where v_k^r, v_k^b, and v_k^e are the measurement errors at time k. The measurement errors have the property

$$E[v_k] = 0, \qquad E[v_j v_k^T] = R_k \delta_{jk}$$

where the measurement noise covariance matrix is defined by

$$R_k = \begin{pmatrix} \sigma_r^2 & 0 & 0 \\ 0 & \sigma_b^2 & 0 \\ 0 & 0 & \sigma_e^2 \end{pmatrix} \tag{4.13}$$

The process noise has the properties

$$E[w_k] = 0, \qquad E[w_j w_k^T] = Q_k \delta_{jk}$$

where the process noise covariance matrix is defined by

$$Q_k = \begin{pmatrix} E_k^x & 0 & 0 \\ 0 & E_k^y & 0 \\ 0 & 0 & E_k^z \end{pmatrix} \tag{4.14}$$

where E_k^x is a diagonal matrix whose elements represent the variance in the Cartesian coordinates of position, velocity, and acceleration, and similarly for E_k^y and E_k^z. These are assumed to be equal, that is,

$$E_k^x = E_k^y = E_k^z = \begin{pmatrix} \sigma_{kp}^2 & 0 & 0 \\ 0 & \sigma_{kv}^2 & 0 \\ 0 & 0 & \sigma_{ka}^2 \end{pmatrix} \tag{4.15}$$

Accordingly, it is assumed that the process noise in position is not correlated with that in velocity or acceleration, etc., and that there is also no noise correlation between the coordinates. The subscripts p, v, and a in (4.15) represent "position", "velocity", and "acceleration".

With the existence of a nonlinear measurements of the state X_k, we must use the Extended Kalman Filter algorithm which handles the case of systems possessing nonlinearities. The basic idea of the Extended Kalman Filter algorithm is linearizing the nonlinear measurement equations about the most recent state estimate, and then implementing the Standard Kalman Filter algorithm which is given by (4.3) through (4.7).

Linearization is obtained by using the first order Taylor series of the nonlinear measurement given in (4.11) about the predicted state estimate $X_{k|k-1}$, giving

$$\tilde{Z}_k = H_k X_k + v_k, \quad H_{kij} = \frac{\partial H_{ki}}{\partial X_{kj}}, \quad H_k = \left. \frac{\partial h_k(X_k)}{\partial X_k} \right|_{X_k = X_{k|k-1}} \tag{4.16}$$

where

$$H_k = \begin{pmatrix} \frac{x_{k|k-1}}{r_{k|k-1}} & 0 & 0 & \frac{yk|k-1}{r_{k|k-1}} & 0 & 0 & \frac{z_{k|k-1}}{r_{k|k-1}} & 0 & 0 \\ -\frac{y_{k|k-1}}{r^2_{k|k-1,h}} & 0 & 0 & \frac{x_{k|k-1}}{r^2_{k|k-1,h}} & 0 & 0 & 0 & 0 & 0 \\ -\frac{z_{k|k-1}x_{k|k-1}}{r_{k|k-1,h}r^2_{k|k-1}} & 0 & 0 & -\frac{z_{k|k-1}y_{k|k-1}}{r_{k|k-1,h}r^2_{k|k-1}} & 0 & 0 & \frac{r_{k|k-1,h}}{r^2_{k|k-1}} & 0 & 0 \end{pmatrix}$$

$$r_{k|k-1} = \sqrt{x^2_{k|k-1} + y^2_{k|k-1} + z^2_{k|k-1}}\,, \qquad r_{k|k-1,h} = \sqrt{x^2_{k|k-1} + y^2_{k|k-1}} \tag{4.17}$$

CHAPTER 5

CALCULATION OF THE MISS DISTANCE

The miss distance (MD) is regarded at the appropriate measure of effectiveness against which the various trajectories discussed in previous chapters are to be compared. These MDs have been estimated only for the conical spiral (CS) trajectories described in chapter 3. It is assumed that the missile state is imprecisely known through measurements of the target's relative distance and direction from the missile. The missile state is estimated by means of Kalman filtering as discussed in Chapter 4. The CS trajectory is obtained by applying an appropriate acceleration at each instant based on the missile's estimated state, according to (3.10). This acceleration is applied to the missile's true state. During the simulation, both the missile's true and estimated states are calculated. Measurements are available only during the CS portion of the trajectory; after transition to Constant Turning Rate no more measurements are possible. The measurements are generated by applying random errors to the true missile position. At the beginning of the trajectory, it is assumed that perfect knowledge of the missile state is available. While this assumption is not realistic and will tend to provide an overoptimistic estimate of the MD, the effects will tend to die out during the course of the missile flight and with the sequence of measurement updates.

Monte Carlo simulations are performed for each set of parameter values. The standard errors in range, bearing, and elevation are denoted by $\sigma_r, \sigma_b, \sigma_e$. Each estimate of MD is based on 100 Monte Carlo experiments.

The parameters determining the MD in each Monte Carlo experiment are as follows:

ϕ_c	Minimum allowed Heading Error (HE)
α_c	Half cone angle in the CS trajectory
v	Missile speed (assumed constant)
a_c	Maximum lateral acceleration capability
dt	Time interval between measurements
σ_r	Standard error in range measurement
σ_b	Standard error in bearing measurement
σ_e	Standard error in elevation measurement
σ_p	Standard process error in position
σ_v	Standard process error in velocity
σ_a	Standard process error in acceleration

Table 5-1 illustrates the effect of measurement rate and angular error on miss distance for the indicated parameter values.

Table 5-1

v	0.5 Mach	a_c	15 g
σ_r	5 m	σ_p^2	3 m^2
σ_v^2	3 m^2s^{-2}	σ_a^2	3 m^2s^{-4}
α_c	15 deg	ϕ_c	10 deg

Values of Miss Distance (m)

$dt \rightarrow$	10 ms	50 ms	80 ms
$\sigma_b = \sigma_e$			
0.3 (deg)	0.3	1.3	3.6
0.5 (deg)	0.5	1.5	4.4
1.0 (deg)	0.9	1.6	4.8
2.0 (deg)	0.8	1.7	5.5
3.0 (deg)	0.8	1.8	6.1
4.0 (deg)	0.7	1.8	6.5
10.0 (deg)	0.6	1.9	7.3

Table 5-2 illustrates the effect of missile speed and minimum heading error.

Table 5-2

a_c	10 g	dt	10 ms
σ_r	5 m	σ_p^2	3 m^2
σ_b	15 deg	σ_v^2	3 m^2s^{-2}
σ_e	15 deg	σ_a^2	3 m^2s^{-4}
α_c	15 deg		

Values of Miss Distance (m)

$v \rightarrow$	0.4 mach	0.5 mach	0.8 mach
ϕ_c			
10 (deg)	0.4	0.9	0.9
15 (deg)	0.8	1.0	1.0

Table 5-3 illustrates the effect of missile speed and minimum heading error.

Table 5-3

a_c	15 g	dt	10 ms
σ_r	5 m	σ_p^2	3 m^2
σ_b	15 deg	σ_v^2	3 m^2s^{-2}
σ_e	15 deg	σ_a^2	3 m^2s^{-4}
α_c	15 deg		

Values of Miss Distance (m)

$v \rightarrow$	0.4 mach	0.5 mach	0.8 mach
ϕ_c			
10 (deg)	0.3	0.5	0.3
15 (deg)	0.3	0.8	0.8

Table 5-4 illustrates the effect of missile speed and limiting lateral acceleration.

Table 5-4

		dt	10 ms
σ_r	5 m	σ_p^2	3 m^2
σ_b	15 deg	σ_v^2	3 m^2s^{-2}
σ_e	15 deg	σ_a^2	3 m^2s^{-4}
α_c	15 deg	ϕ_c	15 deg

Values of Miss Distance (m)

$a_c \rightarrow$	10 g	15 g	20 g
v			
0.4 mach	0.8	0.4	0.4
0.6 mach	1.1	0.9	1.3

Table 5-5 illustrates the effect of missile speed and cone half-angle.

Table 5-5

a_c	15 g	dt	10 ms
σ_r	5 m	σ_p^2	3 m^2
σ_b	15 deg	σ_v^2	3 m^2s^{-2}
σ_e	15 deg	σ_a^2	3 m^2s^{-4}
ϕ_c	15 deg		

Values of Miss Distance (m)

$\alpha_c \rightarrow$	10 deg	15 deg	20 deg
v			
0.4 mach	0.5	0.4	0.4
0.6 mach	0.8	0.9	0.9

Table 5-6 illustrates the effect of limiting lateral acceleration and cone half-angle.

Table 5-6

ϕ_c	15 deg	dt	10 ms
σ_r	5 m	σ_p^2	3 m^2
σ_b	15 deg	σ_v^2	3 m^2s^{-2}
σ_e	15 deg	σ_a^2	3 m^2s^{-4}
v	0.5 mach		

Values of Miss Distance (m)

α_c	$a_c \rightarrow$	10 g	15 g	20 g
10 (deg)		0.4	0.9	0.4
15 (deg)		1.1	0.8	0.6
20 (deg)		0.7	1.0	1.0
30 (deg)		0.8	1.1	1.3

Table 5-7 illustrates the effect of limiting lateral acceleration and heading error.

Table 5-7

α_c	15 deg	dt	10 ms
σ_r	5 m	σ_p^2	3 m^2
σ_b	15 deg	σ_v^2	3 m^2s^{-2}
σ_e	15 deg	σ_a^2	3 m^2s^{-4}
v	0.5 mach		

Values of Miss Distance (m)

ϕ_c	$a_c \rightarrow$	10 g	15 g	20 g
10 (deg)		0.9	0.5	0.4
15 (deg)		0.9	0.8	0.6

CHAPTER 6

SUMMARY AND CONCLUSIONS

Results shown in the previous chapter indicate that missile guidance in the CS trajectory can achieve satisfactorily small miss distances of less than one meter, under appropriate conditions. Reader is cautioned that these results are based only on kinematical studies. If this method is to be pursued it will be necessary to consider missile aerodynamics, which will tend to increase the miss distances.

The process equation used was based on the constant-turning-rate model. This resulted in considerably smaller miss distances than the constant-velocity model, which was initially tried. One might expect somewhat more improvement by modeling the process on the actual CS trajectory being flown.

Experiments with measurement errors of different magnitudes showed that the miss distances are not very sensitive to these errors. However, the miss distances are quite sensitive to the measurement interval. In order for the method to be practical, the measurement interval should be not much greater than 10 ms to achieve miss distances of less than one meter.

CHAPTER 7

REFERENCES

Blair, W. D.; G. A. watson; J. Curry; A. Lepp; G. Pilson; T. Do; M. A. Strock; and Y. Jeleniewski, 1997: Information-Based Radar Resource Allocation: FY96 Test-of-Concept Experiment (TOCE). NSWCDD Technical Report TR-97/22.

Gelb, A., 1974: Applied optimal estimation. MIT Press, Cambridge, MA.

Groves, G. W.; W. D. Blair; and J. E. Gray, 1994: Some concepts for trajectory prediction. NSWCDD Technical Report TR-92/445.

Ohlmeyer, E., 1985: Application of optimal estimation and control concepts to a bank-to-turn missile. NSWCDD Technical Report TR-85/219.

DISTRIBUTION

DOD ACTIVITIES (CONUS)

		Copies
ATTN	DR JULIA ABRAHAMS CODE 311	1
	DR RABINDER MADAN CODE 313	1
	JAMES BUSS CODE 313	1
	JAMES K HALL CODE 313	1
	WILLIAM J MICELI CODE 313	1

OFFICE OF NAVAL RESEARCH
800 N QUINCY ST
ARLINGTON VA 22217-5660

ATTN ROY L STREIT 1
CODE 2002 BUILDING 1171
NAVAL UNDERSEA WARFARE CENTER
1176 HOWELL ST
NEWPORT RI 02841

ATTN DR ROGER OXLEY 1
CODE 5720
NAVAL RESEARCH CENTER
WASHINGTON DC 20375

ATTN DR GERRY TRUNK 1
CODE 5317
RADAR DIVISION
NAVAL RESEARCH CENTER
WASHINGTON DC 20375

ATTN	JOSEPH WILLIAMS	1
	DICK ZIEGLER	1

PMS400B33
NAVAL SEA SYSTEMS COMMAND
2531 JEFFERSON DAVIS HIGHWAY
ARLINGTON VA 22242-5160

ATTN RICHARD BRITTON 1
PMS400BX
NAVAL SEA SYSTEMS COMMAND
2531 JEFFERSON DAVIS HIGHWAY
ARLINGTON VA 22242-5160

ATTN DOUG MARKER 1
PEO-TAD-SET
THEATER AIR DEFENSE
2531 JEFFERSON DAVIS HIGHWAY
ARLINGTON VA 22242-5170

ATTN PASHANG ESFANDIARI 1
PEO-TAD-B
THEATER AIR DEFENSE
2531 JEFFERSON DAVIS HIGHWAY
ARLINGTON VA 22242-5170

ATTN CODE A76 (TECHNICAL LIBRARY) 1
COMMANDING OFFICER
CSSDD NSWC
6703 W HIGHWAY 98
PANAMA CITY FL 32407-7001

DEFENSE TECHNICAL INFO CENTER
8725 JOHN J KINGMAN DRIVE
SUITE 0944
FT BELVOIR VA 22060-6218 1

INTERNAL

		Copies
B05	STATON	1
B20	CHU	1
B30		1
B32		1
B32	ANTHONY	1
B32	CONTE	1
B32	GROVES	5
B32	MCCABE	1
B32	RICE	1
B32	PAULA R WERME	1
B32	WATSON	1
B35	BAILEY	1
B35	FENNEMORE	1
B35	HARRISON	1
B60	TECHNICAL LIBRARY	1
B60A	GRAY	1

DISTRIBUTION (CONTINUED)

G23	J BIBEL	1
G23	GRAFF	1
G23	OHLMEYER	1
G72		1
N05		1
N07	SIMPSON	1
N07	STEVENSON	1
N10		1
N12	ALLENDER	1
N12	HEIN	1
N12	JOHNS	1
N12	KHODARY	5
N12	LAANISTO	1
N12	LE	1
N12	OTTE	1
N12	SCOTT	1
N12	TOY	1
N12	WILLIAMS	1
N14		1
N14	ADDAIR	1
N14	BOYER	1
N14	MURRAY	1
N64	JETER	1
N64	KOUROUKLIS	1
N92		1
N92	LAMBERTSON	1
N92	FOSTER	1
N22	J GRAY	1
T		1
T04		1
T05		1
T20	BEUGLASS	1
T406		1
T41	FONTANA	1
T41	GENTRY	1
T41	MARTIN	1
T41	MIMS	1
T41	PAWLAK	1
T42	CALDWELL	1
T42	CARPENTER	1
T42	KLOCHAK	1
T42	LEONG	1
T50	LUCAS	1